Supplementary Information (SI) for Journal of Materials Chemistry A.
This journal is © The Royal Society of Chemistry 2026

Supplementary Materials

Synergistic defects engineering and cocatalyst loading in Bi_2MoO_6-OVs/MoS_2 photoanode for efficient power generation in H_2O_2 photoelectrochemical cell

Yutong Liu[1], Shuohui Li[1], Bo Yu[2], Yingying Guan[1], Xiaosong Han[1], Yihui Tian[1], Yang Zhao[1,*], Huan Wang[1,*]

[1]College of Chemistry and Chemical Engineering, Northeast Petroleum University, Daqing 163318, China

[2]School of Physics and Optoelectronics, South China University of Technology, Guangzhou 510640, China

[*]Email:

Yang Zhao: yzhao@nepu.edu.cn;

Huan Wang: wanghuan83214@gmail.com

Materials

Analytical grade compounds including Bismuth nitrate pentahydrate ($Bi(NO_3)_3 \cdot 5H_2O$), sodium molybdate dihydrate ($Na_2MoO_4 \cdot 2H_2O$), N, N, N', N'-Tetramethylethylenediamine (TMEDA), ethylene glycol (EG), ethanol, methanol and Ammonium molybdate tetrahydrate ($(NH_4)_2MoS_4$) were acquired from Aladdin Industrial Corporation. Deionized water (DI H_2O) was used during the experiment. All chemicals were analytically pure and did not require further purification.

Material Characterization

Scanning electron microscopy (SEM) and transmission electron microscope (TEM) images were acquired with a Philips XL-30-ESEM-FEG instrument operating at 3 kV and Jem-2100F at an accelerating voltage of 200 kV, respectively. The powder X-ray diffraction (XRD) patterns were obtained on a D/MAX-2200, Japan. Ultraviolet-visible (UV-vis) diffuse reflection spectra (DRS) were measured on a UV-vis spectrophotometer (UV-2550, Shimadzu) with an integrating sphere attachment, and $BaSO_4$ was used as the reference material. X-ray photoelectron spectroscopy (XPS) was taken on the Thermo Fisher Scientific K-Alpha.

Photoelectrochemical measurements

Photoelectrochemical performances were examined by CHI 760E electrochemical workstation (CH Instruments, Chenhua, China) under a three-electrode system in 0.5 M Na_2SO_4 solution by using saturated Ag/AgCl and Pt foil as the reference electrode and counter electrode, respectively. The working electrodes for electrochemical measurements were prepared by dropping the powder samples onto a pre-cleaned

indium doped tin oxide (ITO) glass. In detail, 10 mg of photocatalyst was dispersed in an ethanol solution (260 μL) containing 40 μL of Nafion. After dropping the above mixture on ITO followed by drying at 60 °C, the working electrode was obtained. The Mott-Schottky (M-S) curves were measured in the dark at a frequency of 0.5 kHz, respectively. Electrochemical impedance spectra (EIS) were collected at an off-line potential with frequencies ranging from 105 kHz to 0.1 kHz and modulation amplitude of 5.0 mV. The measured potentials (V *vs.* Ag/AgCl) were converted to the reversible hydrogen electrode (RHE) scale according to the Nernst equation: $E = E_{(Ag/AgCl)} + E^{o}_{(Ag/AgCl)} + 0.059pH$

Characterization of cornstalk-derived porous carbon (PC)

The microstructure and surface morphology of the cornstalk-derived porous carbon (PC) were characterized using SEM. **Fig. S1a** schematically illustrates the hierarchical porous model of PC. The morphology of cornstalk-derived PC exhibited a hierarchical porous layered structure featuring numerous active sites (**Fig. S1b**). XRD patterns of PC revealed two broad diffraction peaks at 22° and 43° [1], assigning to the (002) and (101) planes of amorphous carbon, respectively (**Fig. S1c)**.

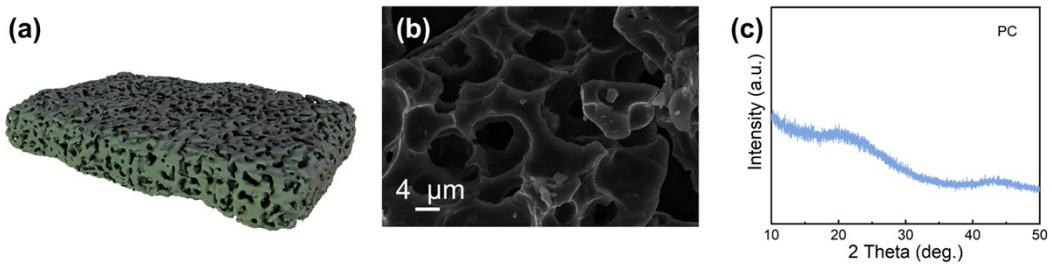

Fig. S1. (a) Structural model, (b) SEM image, and (c) XRD patterns of CSPC.

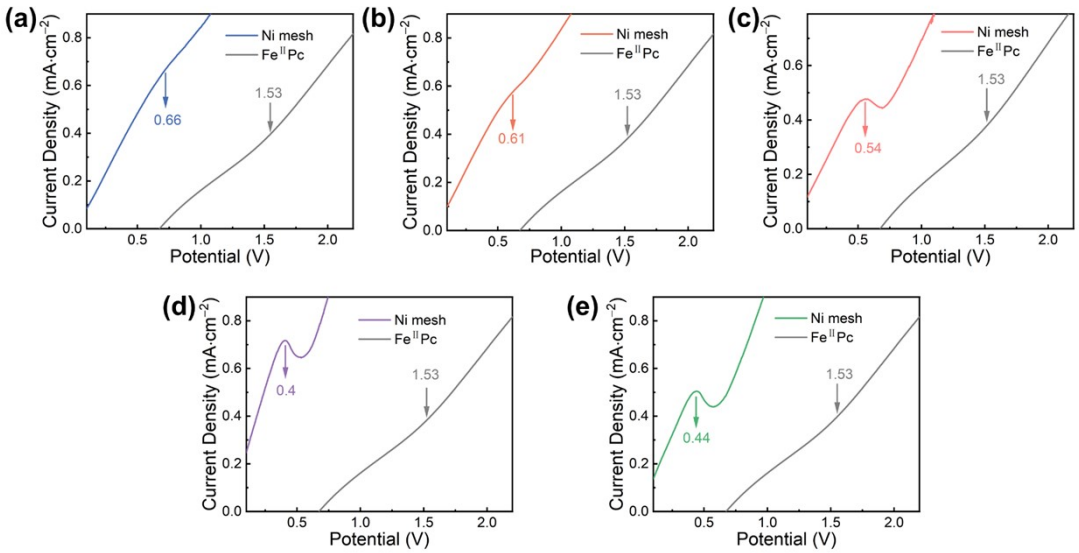

Fig. S2. LSV curves of CSPC/Fe^{II}Pc/ITO cathode and different anodes of BM/Ni mesh (a), BMO/Ni mesh (b), BMOS-1/Ni mesh (c), BMOS-3/Ni mesh (d), and BMOS-5/Ni mesh (e), respectively.

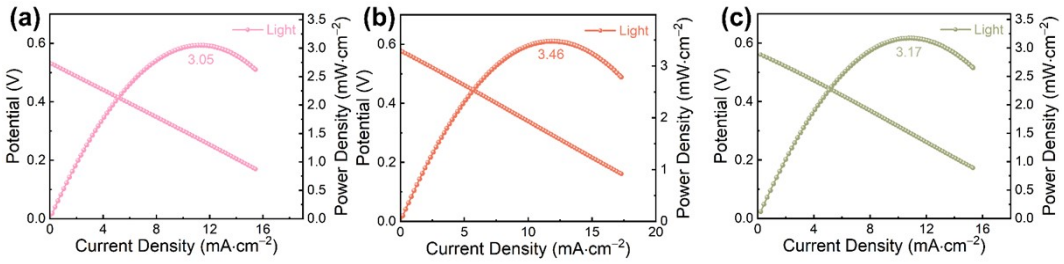

Fig. S3. I-V and I-P curves of (a) BMO-0.3-, (b) BMO-, and (c) BMO-0.7-based cells.

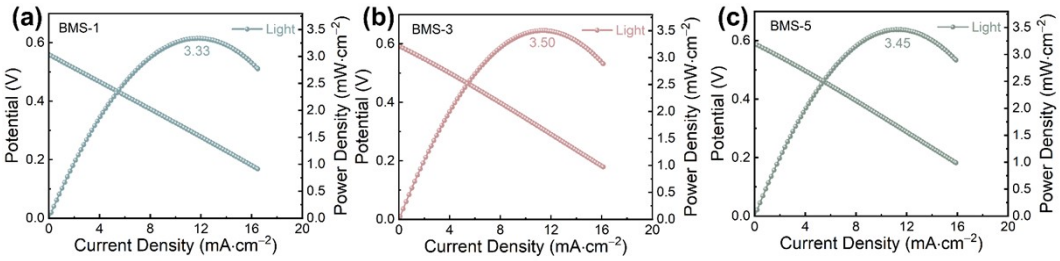

Fig. S4. I-V and I-P curves of (a) BMS-1-, (b) BMS-3-, and (c) BMS-5-based cells.

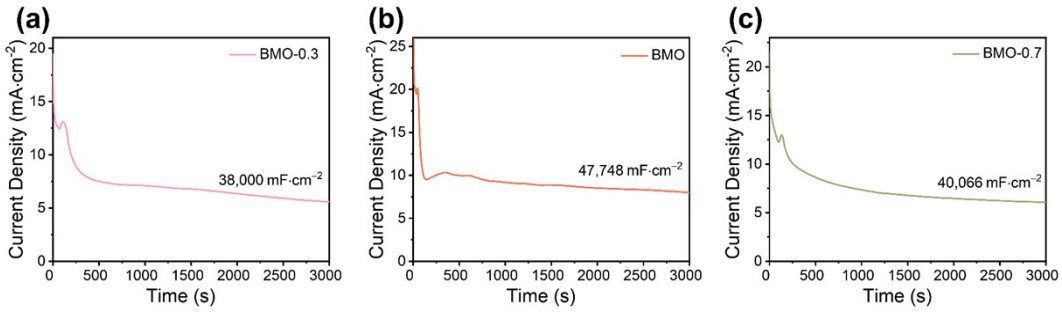

Fig. S5. Specific capacitances of (a) BMO-0.3-, (b) BMO-, and (c) BMO-0.7-based cells after 0.5 h of light irradiation.

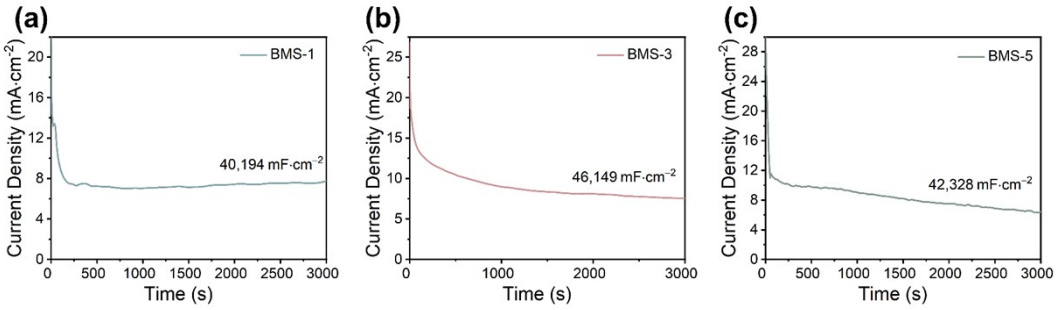

Fig. S6. Specific capacitances of (a) BMS-1-, (b) BMS-3-, and (c) BMS-5-based cells after 0.5 h of light irradiation.

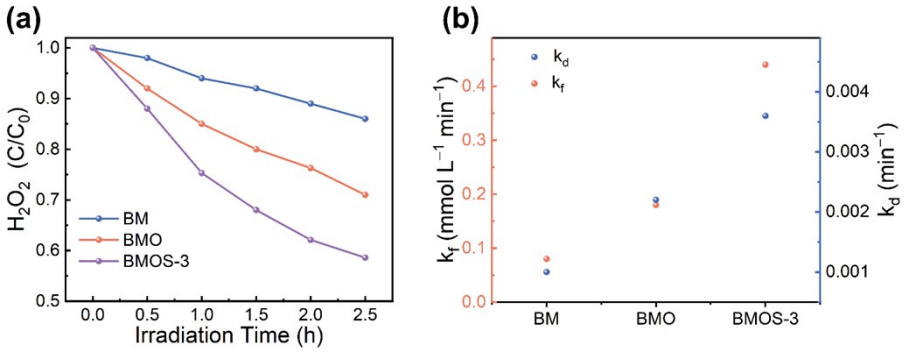

Fig. S7. (a) Photocatalytic decomposition of H_2O_2 over BM, BMO and BMOS-3; (b) Formation rate constant (k_f) and decomposition rate constant (k_d) for photocatalytic H_2O_2 production over the prepared samples.

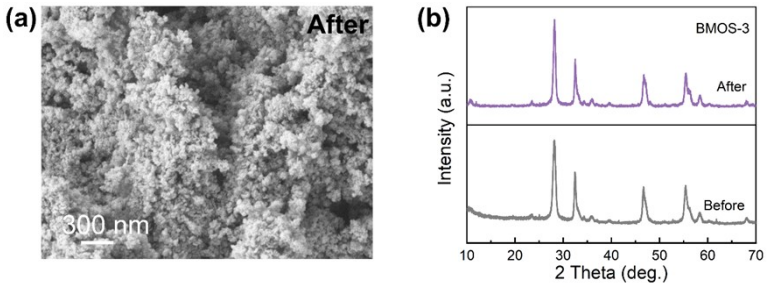

Fig. S8. SEM images of BMOS-3 photoanode after test; (b) XRD patterns of BMOS-3 before and after test.

References

[1] M. Yang, Z. Nie, R. Wang, Y. Zhao, H. Wang, B, N co-doped porous carbon derived from β-cyclodextrin for high-performance supercapacitors, J. Energy Storage 99 (2024) 113271.